





Power Optimization of a Three-Node Two-Way Relay-Assisted Power-Line Communication System

Angie A. G. Liong, *Student Member, IEEE*, Lenin Gopal , *Member, IEEE*, Yue Rong , *Senior Member, IEEE*, Filbert H. Juwono , *Senior Member, IEEE*, and Choo W. R. Chiong , *Member, IEEE*

Abstract— A smart grid system requires two-way communication links. Because power-line infrastructure is widely available, power-line communication (PLC) is preferred as the communication technology in smart grid systems. A power-line, on the other hand, was not designed to carry data and thus suffers from disturbances that attenuate the transmitted signal. Therefore, it is beneficial to provide spatial diversity to improve the system performance. Optimal power allocation has always been an issue to be solved in relay-aided communication systems. Using a two-way multicarrier relay configuration, this paper investigates power optimization of a relay-assisted PLC system with the consideration of the quality of service (QoS) constraints. Further, we investigate the combination of half-duplex and full-duplex nodes. Since the QoS constrained power allocation problem is highly non-convex, an alternating optimization (AO) algorithm is proposed to decompose the optimization problem into sub-problems. The AO algorithm is an iterative algorithm where it uses the newly obtained parameters (e.g., power) to find a new set of other parameters. Simulation results show that the proposed system successfully reduces the total power required by the system compared to the conventional bidirectional direct transmission (BDT) system and the relay-assisted two-way information exchange (R2WX) system under the same QoS requirement.

Index Terms—Power-line communication (PLC), power optimization, three-node two-way relay-assisted (RA), quality of service (QoS).

I. INTRODUCTION

RECENTLY, power-line communication (PLC) has gained much attention along with the rapid development of smart grid systems. Although wireless communications is popular, the

use of PLC is preferred since power-line networks have been well-established, thereby reducing the installation and operational costs. More specifically, the advantages of the PLC system include (1) operational efficiency, (2) minimal deployment cost, (3) extensive coverage, (4) high capacity, and (5) high security [1]. Moreover, two-way data exchange is required between the distribution system operator and the users/prosumers to enable the smart grid applications, such as the automatic meter reading (AMR), etc. [2]–[5].

As PLC technology delivers information data via electrical power-lines with severe channel attenuation, repeaters (relays) can be employed between the transmitter and receiver to improve the system performance [6]. Note that relays have been commonly used in communication systems, especially in wireless communications [7], [8]. Nevertheless, relay characteristics in PLC is different from the ones in wireless communications [9]. In particular, in a relay-assisted PLC system, the signaling paths are highly correlated as they use the same power cable grid whereas in wireless communications, channels of the source, relay, and destination are usually independent of each other. In addition, in PLC systems, the position of the relay nodes and the distance between the transceivers eventually affect the characteristics of the channels and the whole network structure. It is worth mentioning that relay technique has been extensively studied in wireless communications and some algorithms designed for wireless communications may be used for solving the problems in PLC. However, due to the property of channels in PLC, it is still interesting to investigate the relay technique in PLC. In fact, relay technique attracts lots of interests recently in PLC [10], [11].

There are a few types of relay modes for a relay-assisted PLC system to work. For the regenerative scheme or so-called decode-and-forward (DF) relaying, the received signal is first decoded at the relay node before being re-encoded and forwarded to the destination node. Whereas, for the non-regenerative scheme, or so-called amplify-and-forward (AF) relaying, the received signal is simply amplified and then forwarded to the destination. This makes the AF relay scheme having shorter processing delay, and easy to implement as it is less complex.

To date, many research works in relay-assisted PLC (RA-PLC) are available in the literature. It was shown in [12] that increased signal-to-noise ratio (SNR) can be cooperatively achieved by placing a relay device between the transmitter and receiver of a PLC system. Moreover, in [13], it was studied that the achievable data exchange rate of

Manuscript received 4 October 2021; revised 21 February 2022 and 21 April 2022; accepted 5 June 2022. Date of publication 13 June 2022; date of current version 24 January 2023. This work was supported by the Ministry of Higher Education Malaysia through Fundamental Research Grant Scheme (FRGS) under Grant FRGS/1/2016/TK04/CURTIN/02/1. Paper no. TPWRD-01474-2021. (Corresponding author: Lenin Gopal.)

Angie A. G. Liong, Filbert H. Juwono, and Choo W. R. Chiong are with the Department of Electrical and Computer Engineering, Curtin University Malaysia, Miri, Sarawak 98009, Malaysia (e-mail: angie.liong@postgrad.curtin.edu.my; filbert@ieee.org; raymond.ccw@curtin.edu.my).

Lenin Gopal was with the Department of Electrical and Computer Engineering, Curtin University Malaysia, Miri, Sarawak 98009, Malaysia. He is now with the University of Southampton Malaysia (UoSM), Iskandar Puteri, Johor 79100, Malaysia (e-mail: L.Gopal@soton.ac.uk).

Yue Rong is with the School of Electrical Engineering, Computing, and Mathematical Sciences, Curtin University, WA 6102, Australia (e-mail: y.rong@curtin.edu.au).

Color versions of one or more figures in this article are available at <https://doi.org/10.1109/TPWRD.2022.3181297>.

Digital Object Identifier 10.1109/TPWRD.2022.3181297

PLC can be increased by employing two-way AF relay system.

As relays can be considered as transceiver nodes, RA-PLC systems need more power compared to the conventional PLC systems. It is necessary to optimize the power usage to meet the system requirement and to establish green communications infrastructure. In [14], two-way AF relay system for indoor PLC network was optimized with QoS consideration. The system model discussed in [14] consisted of two terminals with a relay between them. In other words, the direct link between the source and destination nodes was not available in this system. In contrast, a direct link in the RA-PLC system was presented in [15]. The system was optimized for the source and relay power allocation in a general broadcast-and-multiaccess (BMA) multicarrier relay transmission system to minimize the total power consumption. In [15], a time-division duplexing (TDD) mode was assumed and no reverse channels were discussed. Furthermore, the authors used AF relay-involved PLC system to achieve both time and spatial diversity [16]. Note that in a BMA mode, the signal is broadcasted by the source node to the other two nodes in the first transmission phase. In the second phase, the source node continues to broadcast while the relay node forwards its received signal to the destination node. In addition, it has been shown that the two-way relay (TWR) systems can effectively support data exchange within the two phases in BMA [17], [18].

As mentioned previously, smart grid systems need two-way communication links. To the best of our knowledge, two-way power-optimized RA-PLC systems with direct link between the source and destination terminal nodes and with hybrid half and full duplex nodes have not been discussed in the existing research works. To emphasize, although the problems and methods are similar with [14], the derivation and solution is not straightforward as the system in [14] does not have the direct link between the source and destination nodes. It is worth mentioning that it is beneficial to include a direct link in a communication system under harsh channels to provide spatial diversity, thereby improving the system performance [19]. Furthermore, the nature of a PLC system is half-duplex as the communication uses the same cable [20]. Currently, full-duplex PLC has been proposed to outperform the performance of the half-duplex system [21]. In this paper, we incorporate both half-duplex and full-duplex nodes to better visualize the practical PLC system.

To fill the above-mentioned gaps, in this paper we propose a power optimization scheme for a three-node two-way RA BMA multicarrier indoor PLC network with consideration of quality of service (QoS) constraints by combining both half-duplex and full-duplex nodes. In practical environment, PLC systems need to emit lower electromagnetic interference (EMI) at lower transmission power to reduce the interference to other applications. Thus, the QoS criteria have to be set to the lower-bound of the data traffic capacity. Since the QoS constrained power allocation problem is highly non-convex, the alternating optimization (AO) algorithm is used to decompose the optimization problem to sub-problems. In particular, we first build the system model of the proposed system and then introduce the protocol of the forward and reverse network operations. Next, mathematical problems are derived and solved by using the

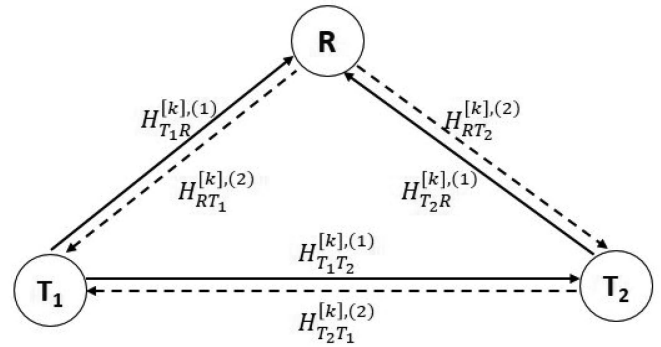


Fig. 1. A three-node two-way relay system model where the solid-lines indicate first phase and the dash-line indicate the second phase.

Karush-Kuhn-Tucker (KKT) conditions and the AO algorithm. Numerical examples are shown through simulations. Simulation results show the proposed system is able to reduce the total power required by the system for about 40% compared to the conventional bidirectional direct transmission (BDT) system under the same QoS requirement. In summary, the contributions of this paper are twofold:

- 1) We propose a two-way RA-PLC system with the direct link between the source and destination terminal nodes by incorporating both half-duplex and full-duplex nodes in the system.
- 2) We derive power optimization problems, solve them using the KKT conditions and the AO algorithm and compare the performance with the conventional BDT and R2WX systems.

The rest of the paper is organized as follows, in Section II, the system model is presented and the problem is formulated. Section III describes the three sub-problems formulated from Section II, their optimization procedures, and the AO algorithm. The performance of the proposed algorithm is illustrated in Section IV. Conclusions are presented in Section V.

II. SYSTEM MODEL AND PROBLEM FORMULATION

A multicarrier three-node two-way PLC system with a source node (T_1), a relay node (R) and a destination node (T_2) is depicted in Fig. 1. We assume that orthogonal frequency-division multiplexing (OFDM) is employed as the modulation technique. The available system bandwidth, B is divided uniformly into K subcarriers so that the channel fading can be considered as flat at each subcarrier. The channel frequency response (CFR) at the k -th ($k = 1, 2, \dots, K$) subcarrier from node L_1 to node L_2 during the n -th phase ($n = 1, 2$) is denoted by $H_{L_1L_2}^{[k],[n]}$, where $L_1, L_2 \in \{T_1, T_2, R\}$.

Furthermore, we assume that the source node and relay node operate in half-duplex mode where the nodes are allowed to either transmit or receive signal at one particular time. On the contrary, we assume that the destination node employs an ideal circulator. As a result, it is able to operate in in-band full-duplex mode, i.e. it can transmit and receive at the same time and over the same frequency, with negligible self-interference [22], [23].

Finally, for the sake of simplicity, we assume that the loads and channel are matched, so that there are no multipath reflections.

The proposed protocol can be explained as follows. In the first phase, the source node T_1 broadcasts signal $X_1^{[k]}$ to R and T_2 while the destination node T_2 transmits signal $X_2^{[k]}$ to R . In the second phase, the node R amplifies and broadcasts the received signals to T_1 and T_2 . At the same time, T_2 transmits X_2 to T_1 . To avoid confusion, from now on we avoid using the ‘source node’ and ‘destination node’ terms and we refer data flow $T_1 \rightarrow (R) \rightarrow T_2$ as the *forward mode* while the flow $T_1 \leftarrow (R) \leftarrow T_2$ as the *reverse mode*.

We assume that $X_1^{[k]}$ and $X_2^{[k]}$ follow Gaussian distribution with zero mean and unit variance. Let the transmission power at the k -th subcarrier from T_1 be $P_{T_1}^{[k]}$, from T_2 be $P_{T_2}^{[k]}$, and from R be $P_R^{[k]}$. In the forward mode, node T_1 broadcasts the signal $X_1^{[k]}$ with power $P_{T_1}^{[k]}$. On the other hand, in the reverse mode, node T_2 broadcasts $X_2^{[k]}$ with power $P_{T_2,1}^{[k]}$ and $P_{T_2,2}^{[k]}$ in the first and second phase, respectively. The total transmit power of node T_2 is given by

$$P_{T_2}^{[k]} = P_{T_2,1}^{[k]} + P_{T_2,2}^{[k]}. \quad (1)$$

Therefore, the total network power is given by

$$P_{\Sigma} = \sum_{k=1}^K P_{T_1}^{[k]} + \sum_{k=1}^K P_{T_2}^{[k]} + \sum_{k=1}^K P_R^{[k]}. \quad (2)$$

As the broadcasting nature of the power-line makes the received signal in relay node and destination node have different channel gain and noise disturbances, the received signals in the first phase can be mathematically modeled as

$$Y_{R,1}^{[k]} = H_{T_1 R}^{[k],(1)} \sqrt{P_{T_1}^{[k]}} X_1^{[k]} + H_{T_2 R}^{[k],(1)} \sqrt{P_{T_2,1}^{[k]}} X_2^{[k]} + N_R^{[k]}, \quad (3)$$

$$Y_{T_2,1}^{[k]} = H_{T_1 T_2}^{[k],(1)} \sqrt{P_{T_1}^{[k]}} X_1^{[k]} + N_{T_2,1}^{[k]}, \quad (4)$$

where $Y_{L,1}^{[k]}$ and $N_L^{[k]}$ represent the received signal in the first phase at node L and the noise at node L where $L \in \{R, T_2\}$; while $N_{T_2,1}^{[k]}$ denotes the k th subchannel noise at the destination node in the first phase. Following [14], we assume that the power spectral density (PSD) of noise is the same for each node between two successive phases.

In the second phase, the relay node amplifies the received signal with amplitude gain $g^{[k]}$, then it broadcasts the amplified signal to node T_1 and to node T_2 with power $P_R^{[k]}$. The received signals in the second phase can be mathematically modeled by

$$Y_{T_1,2}^{[k]} = H_{RT_1}^{[k],(2)} g^{[k]} Y_{R,1}^{[k]} + H_{T_2 T_1}^{[k],(2)} \sqrt{P_{T_2,2}^{[k]}} X_2^{[k]} + N_{T_1}^{[k]}, \quad (5)$$

$$Y_{T_2,2}^{[k]} = H_{RT_2}^{[k],(2)} g^{[k]} Y_{R,1}^{[k]} + N_{T_2,2}^{[k]}, \quad (6)$$

where $Y_{L,2}^{[k]}$ represents the received signal in the second phase at node L where $L \in \{T_1, T_2\}$; while $N_{T_2,2}^{[k]}$ denotes the k th subchannel noise at the destination node in the second phase.

The gain $g^{[k]}$ can be expressed as

$$g^{[k]} = \sqrt{\frac{P_R^{[k]}}{P_{T_1}^{[k]} |H_{T_1 R}^{[k],(1)}|^2 + P_{T_2,1}^{[k]} |H_{T_2 R}^{[k],(1)}|^2 + W^{[k]}}}, \quad (7)$$

where $W^{[k]}$ is the noise power.

Substituting (3) into (5) and (6) gives

$$\begin{aligned} Y_{T_1,2}^{[k]} &= \left(H_{T_1 R}^{[k],(1)} H_{RT_1}^{[k],(2)} g^{[k]} \sqrt{P_{T_1}^{[k]}} \right) X_1^{[k]} \\ &\quad + \left(H_{T_2 R}^{[k],(1)} H_{RT_1}^{[k],(2)} g^{[k]} \sqrt{P_{T_2,1}^{[k]}} + H_{T_2 T_1}^{[k],(2)} \sqrt{P_{T_2,2}^{[k]}} \right) X_2^{[k]} + H_{RT_1}^{[k],(2)} g^{[k]} N_R^{[k]} \\ &\quad + N_{T_1}^{[k]}, \end{aligned} \quad (8)$$

and

$$\begin{aligned} Y_{T_2,2}^{[k]} &= \left(H_{T_1 R}^{[k],(1)} H_{RT_2}^{[k],(2)} g^{[k]} \sqrt{P_{T_1}^{[k]}} \right) X_1^{[k]} \\ &\quad + \left(H_{T_2 R}^{[k],(1)} H_{RT_2}^{[k],(2)} g^{[k]} \sqrt{P_{T_2,1}^{[k]}} \right) X_2^{[k]} \\ &\quad + H_{RT_2}^{[k],(2)} g^{[k]} N_R^{[k]} + N_{T_2,2}^{[k]}. \end{aligned} \quad (9)$$

It is assumed that the channel state information (CSI) is available to the nodes. Since T_1 has full knowledge of $X_1^{[k]}$, the first term in (8) can be readily eliminated and the remaining term is used to decode the information of signal $X_2^{[k]}$. Similarly, the second term in (9) is eliminated and the remaining term is used to decode the information of signal $X_1^{[k]}$. The SNRs at T_1 , and two phases of T_2 (denotes as $T_{2,1}$ and $T_{2,2}$) can be derived as

$$SNR_{T_1} = \frac{\left(\sqrt{\sigma v} + \sqrt{\phi(1 + \rho + v)} \right)^2}{1 + \rho + v + \sigma}, \quad (10)$$

$$SNR_{T_{2,1}} = \varrho, \quad (11)$$

$$SNR_{T_{2,2}} = \frac{\tau \rho}{1 + \rho + v + \tau}, \quad (12)$$

where

$$\rho = P_{T_1}^{[k]} \lambda_{T_1 R}^{[k],(1)},$$

$$\varrho = P_{T_1}^{[k]} \lambda_{T_1 T_2}^{[k],(1)},$$

$$\sigma = P_R^{[k]} \lambda_{RT_1}^{[k],(2)},$$

$$\tau = P_R^{[k]} \lambda_{RT_2}^{[k],(2)},$$

$$v = P_{T_2,1}^{[k]} \lambda_{T_2 R}^{[k],(1)},$$

$$\phi = P_{T_2,2}^{[k]} \lambda_{T_2 T_1}^{[k],(2)},$$

and the normalized path gain from node L_1 to L_2 in the n -th ($n = 1, 2$) phase is given by

$$\lambda_{L_1 L_2}^{[k],(n)} = \frac{|H_{L_1 L_2}^{[k],(n)}|^2}{W^{[k]}}. \quad (13)$$

The detailed derivations can be found in Appendices A, B, C.

The average sub-channel capacity (ASC) in bits/s/Hz of the data traffic from T_2 to T_1 and from T_1 to T_2 are respectively given by

$$\bar{C}_1 = \frac{1}{2K} \sum_{k=1}^K \log_2(1 + SNR_{T_1}),$$

$$\bar{C}_2 = \frac{1}{2K} \sum_{k=1}^K \log_2(1 + SNR_{T_{2,1}} + SNR_{T_{2,2}}).$$

Note that the factor $\frac{1}{2}$ appears due to the two-phase system.

By applying QoS criteria as the lower-bound of the system capacity, we formulate an optimization problem to make the most efficient utilization of the system total power as follows

$$\min_{P_{T_1}^{[k]}, P_{T_2}^{[k]}, P_R^{[k]}} P_\Sigma \quad (14a)$$

subject to

$$\bar{C}_1 \geq \bar{q}_1, \quad (14b)$$

$$\bar{C}_2 \geq \bar{q}_2, \quad (14c)$$

$$P_{T_1}^{[k]}, P_{T_2}^{[k]}, P_R^{[k]} \geq 0, \quad \forall k, \quad (14d)$$

where (14a) is the objective function of the total network transmission power, and both \bar{q}_1 and \bar{q}_2 show the minimal link capacity required to support the smart grid applications.

As the optimization problem is non-convex, the exact solution to the optimization problem is hard to obtain. Thus, an alternating optimization approach is proposed by firstly optimizing $P_R^{[k]}$ given $P_{T_1}^{[k]}$, $P_{T_{2,1}}^{[k]}$ and $P_{T_{2,2}}^{[k]}$ values. We then optimize $P_{T_1}^{[k]}$ given $P_{T_{2,1}}^{[k]}$ and $P_{T_{2,2}}^{[k]}$ as well as the previously optimized $P_R^{[k]}$. Next, we optimize $P_{T_{2,1}}^{[k]}$ given $P_{T_{2,2}}^{[k]}$ and the previously optimized $P_{T_1}^{[k]}$ and $P_R^{[k]}$. The last step is to optimize $P_{T_{2,2}}^{[k]}$ given the previously optimized $P_R^{[k]}$, $P_{T_1}^{[k]}$ and $P_{T_{2,1}}^{[k]}$. The process is repeated until convergence, i.e., the difference between the total power obtained in two successive iterations is less than a certain threshold. The resulting sub-problems are convex for any groups of power allocation variables with the remaining variables fixed. Thus, an alternating algorithm is developed to solve the problem (14a)–(14d) which will be discussed in the following subsections.

III. OPTIMIZATION PROBLEMS

A. Optimal Relay Power Allocation Given Source Power Allocations

Using the given initial values of $P_{T_1}^{[k]}$, $P_{T_{2,1}}^{[k]}$ and $P_{T_{2,2}}^{[k]}$, the problem (14a)–(14d) become

$$\min_{P_R^{[k]}} \sum_{k=1}^K P_R^{[k]}, \quad (15a)$$

subject to

$$2K\bar{q}_1 - \sum_{k=1}^K \log_2 \left(A_k + \frac{B_k + C_k \sqrt{P_R^{[k]}}}{D_k P_R^{[k]} + E_k} \right) \leq 0, \quad (15b)$$

$$2K\bar{q}_2 - \sum_{k=1}^K \log_2 \left(F_k - \frac{G_k}{H_k P_R^{[k]} + E_k} \right) \leq 0, \quad (15c)$$

$$P_R^{[k]} \geq 0, \forall k, \quad (15d)$$

where

$$A_k = 1 + P_{T_{2,1}}^{[k]} \lambda_{T_2 R}^{[k],(1)},$$

$$B_k = \left(P_{T_{2,2}}^{[k]} \lambda_{T_2 T_1}^{[k],(2)} - P_{T_{2,1}}^{[k]} \lambda_{T_2 R}^{[k],(1)} \right) E_k$$

$$C_k = 2\sqrt{P_{T_{2,1}}^{[k]} \lambda_{T_2 R}^{[k],(1)} P_{T_{2,2}}^{[k]} \lambda_{T_2 T_1}^{[k],(2)} \lambda_{RT_1}^{[k],(2)}} \times \sqrt{E_k}$$

$$D_k = \lambda_{RT_1}^{[k],(2)},$$

$$E_k = 1 + P_{T_1}^{[k]} \lambda_{T_1 R}^{[k],(1)} + P_{T_{2,1}}^{[k]} \lambda_{T_2 R}^{[k],(1)},$$

$$F_k = 1 + P_{T_1}^{[k]} \lambda_{T_1 R}^{[k],(1)} + P_{T_1}^{[k]} \lambda_{T_1 T_2}^{[k],(1)},$$

$$G_k = P_{T_1}^{[k]} \lambda_{T_1 R}^{[k],(1)} E_k,$$

$$H_k = \lambda_{RT_2}^{[k],(2)}.$$

Applying Karush-Kuhn-Tucker (KKT) conditions to the problem (15a)–(15d) results in the expressions (16a)–(16e) shown at the bottom of the next page.

Proposition 1: The problem (15a)–(15d) becomes convex with the condition of $\{P_R^{[k]} | P_R^{[k]} \geq 0\}$. When $\alpha_1, \alpha_2 > 0$, the left-hand side (LHS) of (16a)–(16d) are monotonic functions of $P_R^{[k]}$. Thus, a bi-section search algorithm may be used to solve (16a)–(16e), which is also the solution of the problem (15a)–(15d).

B. Optimal First Terminal Power Allocation Given Second Terminal and Relay Power Allocations

Using the newly optimized value $P_R^{[k]}$ and the given initial value $P_{T_{2,1}}^{[k]}$ and $P_{T_{2,2}}^{[k]}$, the problem (14a)–(14d) becomes

$$\min_{P_{T_1}^{[k]}} \sum_{k=1}^K P_{T_1}^{[k]}, \quad (17a)$$

subject to

$$2K\bar{q}_1 - \sum_{k=1}^K \log_2 \left(I_k + \frac{J_k + K_k \sqrt{L_k + M_k P_{T_1}^{[k]}}}{M_k P_{T_1}^{[k]} + N_k} \right) \leq 0, \quad (17b)$$

$$2K\bar{q}_2 - \sum_{k=1}^K \log_2 \left(O_k + Q_k P_{T_1}^{[k]} - \frac{R_k}{M_k P_{T_1}^{[k]} + S_k} \right) \leq 0, \quad (17c)$$

$$P_{T_1}^{[k]} \geq 0, \quad \forall k, \quad (17d)$$

where

$$I_k = 1 + P_{T_{2,2}}^{[k]} \lambda_{T_2 T_1}^{[k],(2)},$$

$$J_k = P_R^{[k]} \lambda_{RT_1}^{[k],(2)} \left(P_{T_{2,1}}^{[k]} \lambda_{T_2 R}^{[k],(1)} - P_{T_{2,2}}^{[k]} \lambda_{T_2 T_1}^{[k],(2)} \right),$$

$$K_k = 2\sqrt{P_R^{[k]} \lambda_{RT_1}^{[k],(2)} P_{T_{2,1}}^{[k]} \lambda_{T_2 R}^{[k],(1)} P_{T_{2,2}}^{[k]} \lambda_{T_2 T_1}^{[k],(2)}},$$

$$L_k = 1 + P_{T_{2,1}}^{[k]} \lambda_{T_2 R}^{[k],(1)},$$

$$M_k = \lambda_{T_1 R}^{[k],(1)},$$

$$N_k = 1 + P_R^{[k]} \lambda_{RT_1}^{[k],(2)} + P_{T_{2,1}}^{[k]} \lambda_{T_2 R}^{[k],(1)},$$

$$O_k = 1 + P_R^{[k]} \lambda_{RT_2}^{[k],(2)},$$

$$Q_k = \lambda_{T_1 T_2}^{[k],(1)},$$

$$R_k = P_R^{[k]} \lambda_{RT_2}^{[k],(2)} \left(1 + P_R^{[k]} \lambda_{RT_2}^{[k],(2)} + P_{T_{2,1}}^{[k]} \lambda_{T_2 R}^{[k],(1)} \right),$$

$$S_k = 1 + P_R^{[k]} \lambda_{RT_2}^{[k],(2)} + P_{T_{2,1}}^{[k]} \lambda_{T_2 R}^{[k],(1)}.$$

Similar to Section III-A, we apply KKT conditions to the problem (17a)–(17d) to have the expressions (18a)–(18e) shown at the bottom of the next page.

Proposition 2: The problem (17a)–(17d) becomes convex with the condition of $\{P_{T_1}^{[k]} | P_{T_1}^{[k]} \geq 0\}$. When $\beta_1, \beta_2 > 0$, the LHS of (18a)–(18c) are monotonic functions of $P_{T_1}^{[k]}$. A bisection search algorithm may be used to solve (18a)–(18e), which is also the solution of the problem (17a)–(17d).

C. Optimal Second Terminal Power Allocation of First Phase Given First Terminal and Relay Power Allocations

Using the newly optimized value $P_R^{[k]}$ and $P_{T_1}^{[k]}$ obtained from the Sections III-A to III-B and the given initial value $P_{T_{2,2}}^{[k]}$, the problem (14a)–(14d) becomes

$$\min_{P_{T_{2,1}}^{[k]}} \sum_{k=1}^K P_{T_{2,1}}^{[k]}, \quad (19a)$$

subject to

$$2K\bar{q}_1 - \sum_{k=1}^K \log_2 \left(T_k + \frac{U_k + V_k \sqrt{P_{T_{2,1}}^{[k]} (X_k + Y_k P_{T_{2,1}}^{[k]})}}{Y_k P_{T_{2,1}}^{[k]} + Z_k} \right) \leq 0, \quad (19b)$$

$$2K\bar{q}_2 - \sum_{k=1}^K \log_2 \left(a_k + \frac{b_k}{Y_k P_{T_{2,1}}^{[k]} + c_k} \right) \leq 0, \quad (19c)$$

$$P_{T_{2,1}}^{[k]} \geq 0, \quad \forall k, \quad (19d)$$

where

$$T_k = 1 + P_R^{[k]} \lambda_{RT_1}^{[k],(2)} + P_{T_{2,2}}^{[k]} \lambda_{T_2 T_1}^{[k],(2)},$$

$$U_k = -P_R^{[k]} \lambda_{RT_1}^{[k],(2)} (Z_k + P_{T_{2,2}}^{[k]} \lambda_{T_2 T_1}^{[k],(2)}),$$

$$V_k = 2\sqrt{P_R^{[k]} \lambda_{RT_1}^{[k],(2)} \lambda_{T_2 R}^{[k],(1)} P_{T_{2,2}}^{[k]} \lambda_{T_2 T_1}^{[k],(2)}},$$

$$X_k = 1 + P_{T_1}^{[k]} \lambda_{T_1 R}^{[k],(1)},$$

$$Y_k = \lambda_{T_2 R}^{[k],(1)},$$

$$Z_k = 1 + P_{T_1}^{[k]} \lambda_{T_1 R}^{[k],(1)} + P_R^{[k]} \lambda_{RT_1}^{[k],(2)},$$

$$1 + \alpha_1 \frac{C_k D_k P_R^{[k]} + 2B_k D_k \sqrt{P_R^{[k]}} - C_k E_k}{2 \ln(2) \left(A_k D_k P_R^{[k]} + A_k E_k + C_k \sqrt{P_R^{[k]}} + B_k \right) \sqrt{P_R^{[k]}} (D_k P_R^{[k]} + E_k)} - \alpha_2 \frac{G_k H_k}{\ln(2) \left(F_k - \frac{G_k}{H_k P_R^{[k]} + E_k} \right) (H_k P_R^{[k]} + E_k)^2} = 0 \quad (16a)$$

$$\alpha_1 \left[2K\bar{q}_1 - \sum_{k=1}^K \log_2 \left(A_k + \frac{B_k + C_k \sqrt{P_R^{[k]}}}{D_k P_R^{[k]} + E_k} \right) \right] = 0 \quad (16b)$$

$$\alpha_2 \left[2K\bar{q}_2 - \sum_{k=1}^K \log_2 \left(F_k - \frac{G_k}{H_k P_R^{[k]} + E_k} \right) \right] = 0 \quad (16c)$$

$$\alpha_1, \alpha_2 \geq 0 \quad (16d)$$

$$P_R^{[k]} \geq 0 \quad (16e)$$

$$\begin{aligned}
a_k &= 1 + P_{T_1}^{[k]} \lambda_{T_1 T_2}^{[k],(1)}, \\
b_k &= P_R^{[k]} \lambda_{RT_2}^{[k],(2)} P_{T_1}^{[k]} \lambda_{T_1 R}^{[k],(1)}, \\
c_k &= 1 + P_R^{[k]} \lambda_{RT_2}^{[k],(2)} + P_{T_1}^{[k]} \lambda_{T_1 R}^{[k],(1)}.
\end{aligned}$$

After applying KKT conditions to the problem (19a)–(19d), we have (20a)–(20e) shown as the bottom of this page.

Proposition 3: The problem (19a)–(19d) becomes convex with the condition of $\{P_{T_{2,1}}^{[k]} | P_{T_{2,1}}^{[k]} \geq 0\}$. When $\gamma_1, \gamma_2 > 0$, the LHS of (20a)–(20c) are monotone functions of $P_{T_{2,1}}^{[k]}$. Once again, a bi-section search algorithm may be used to solve (20a)–(20e), which is also the solution of the problem (19a)–(19d).

D. Optimal Second Terminal Power Allocation of Second Phase Given First Terminal and Relay Power Allocations

Using the newly optimized value $P_R^{[k]}$, $P_{T_1}^{[k]}$ and $P_{T_{2,1}}^{[k]}$ obtained from Sections III-A to III-C, the problem (14a)–(14d) becomes

$$\min_{P_{T_{2,2}}^{[k]}} \sum_{k=1}^K P_{T_{2,2}}^{[k]}, \quad (21a)$$

subject to

$$2K\bar{q}_1 - \sum_{k=1}^K \log_2(\Psi_k) \leq 0, \quad (21b)$$

$$\begin{aligned}
1 + \beta_1 &\frac{M_k \left(K_k M_k P_{T_1}^{[k]} + 2J_k \sqrt{M_k P_{T_1}^{[k]} + L_k} + 2K_k L_k - K_k N_k \right)}{2 \ln(2) \left(I_k M_k P_{T_1}^{[k]} + K_k \sqrt{M_k P_{T_1}^{[k]} + L_k} + I_k N_k + J_k \right) \sqrt{M_k P_{T_1}^{[k]} + L_k} \left(M_k P_{T_1}^{[k]} + N_k \right)} \\
&- \beta_2 \frac{Q_k + \frac{R_k M_k}{(M_k P_{T_1}^{[k]} + S_k)^2}}{\ln(2) \left(O_k + Q_k P_{T_1}^{[k]} - \frac{R_k}{M_k P_{T_1}^{[k]} + S_k} \right)} = 0 \quad (18a)
\end{aligned}$$

$$\beta_1 \left[2K\bar{q}_1 - \sum_{k=1}^K \log_2 \left(I_k + \frac{J_k + K_k \sqrt{L_k + M_k P_{T_1}^{[k]}}}{M_k P_{T_1}^{[k]} + N_k} \right) \right] = 0 \quad (18b)$$

$$\beta_2 \left[2K\bar{q}_2 - \sum_{k=1}^K \log_2 \left(O_k + Q_k P_{T_1}^{[k]} - \frac{R_k}{M_k P_{T_1}^{[k]} + S_k} \right) \right] = 0 \quad (18c)$$

$$\beta_1, \beta_2 \geq 0 \quad (18d)$$

$$P_{T_1}^{[k]} \geq 0 \quad (18e)$$

$$\begin{aligned}
1 + \gamma_1 &\frac{V_k X_k Y_k P_{T_{2,1}}^{[k]} - 2V_k Y_k Z_k P_{T_{2,1}}^{[k]} - V_k X_k Z_k + 2U_k Y_k \sqrt{P_{T_{2,1}}^{[k]} (Y_k P_{T_{2,1}}^{[k]} + X_k)}}{2 \ln(2) \left(T_k Y_k P_{T_{2,1}}^{[k]} + V_k \sqrt{P_{T_{2,1}}^{[k]} (Y_k P_{T_{2,1}}^{[k]} + X_k)} + T_k Z_k + U_k \right) \sqrt{P_{T_{2,1}}^{[k]} (Y_k P_{T_{2,1}}^{[k]} + X_k)} (Y_k P_{T_{2,1}}^{[k]} + Z_k)} \\
&+ \gamma_2 \frac{b_k Y_k}{\ln(2) \left(a_k + \frac{b_k}{Y_k P_{T_{2,1}}^{[k]} + c_k} \right) (Y_k P_{T_{2,1}}^{[k]} + c_k)^2} = 0 \quad (20a)
\end{aligned}$$

$$\gamma_1 \left[2K\bar{q}_1 - \sum_{k=1}^K \log_2 \left(T_k + \frac{U_k + V_k \sqrt{P_{T_{2,1}}^{[k]} (X_k + Y_k P_{T_{2,1}}^{[k]})}}{Y_k P_{T_{2,1}}^{[k]} + Z_k} \right) \right] = 0 \quad (20b)$$

$$\gamma_2 \left[2K\bar{q}_2 - \sum_{k=1}^K \log_2 \left(a_k + \frac{b_k}{Y_k P_{T_{2,1}}^{[k]} + c_k} \right) \right] = 0 \quad (20c)$$

$$\gamma_1, \gamma_2 \geq 0 \quad (20d)$$

$$P_{T_{2,1}}^{[k]} \geq 0 \quad (20e)$$

$$P_{T_{2,2}}^{[k]} \geq 0, \quad \forall k, \quad (21c)$$

where

$$\begin{aligned} \Psi_k &= 1 + d_k + e_k P_{T_{2,2}}^{[k]} + f_k \sqrt{P_{T_{2,2}}^{[k]}}, \\ d_k &= \frac{P_R^{[k]} \lambda_{RT_1}^{[k),(2)} P_{T_{2,1}}^{[k]} \lambda_{T_2 R}^{[k),(1)}}{1 + P_{T_1}^{[k]} \lambda_{T_1 R}^{[k),(1)} + P_{T_{2,1}}^{[k),(1)} \lambda_{T_2 R}^{[k),(1)} + P_R^{[k]} \lambda_{RT_1}^{[k),(2)}}, \\ e_k &= \frac{\lambda_{T_2 T_1}^{[k),(2)} \left(1 + P_{T_1}^{[k]} \lambda_{T_1 R}^{[k),(1)} + P_{T_{2,1}}^{[k),(1)} \lambda_{T_2 R}^{[k),(1)} \right)}{1 + P_{T_1}^{[k]} \lambda_{T_1 R}^{[k),(1)} + P_{T_{2,1}}^{[k),(1)} \lambda_{T_2 R}^{[k),(1)} + P_R^{[k]} \lambda_{RT_1}^{[k),(2)}}, \\ f_k &= \frac{2 \sqrt{P_R^{[k]} \lambda_{RT_1}^{[k),(2)} P_{T_{2,1}}^{[k),(1)} \lambda_{T_2 R}^{[k),(1)} \lambda_{T_2 T_1}^{[k),(2)}}}{1 + P_{T_1}^{[k]} \lambda_{T_1 R}^{[k),(1)} + P_{T_{2,1}}^{[k),(1)} \lambda_{T_2 R}^{[k),(1)} + P_R^{[k]} \lambda_{RT_1}^{[k),(2)}} \times \\ &\quad \sqrt{\left(1 + P_{T_1}^{[k]} \lambda_{T_1 R}^{[k),(1)} + P_{T_{2,1}}^{[k),(1)} \lambda_{T_2 R}^{[k),(1)} \right)}. \end{aligned}$$

After applying KKT conditions to the problem (21a)–(21c), the solutions for the problem can be written as

$$1 - \delta_1 \frac{2e_k \sqrt{P_{T_{2,2}}^{[k]} + f_k}}{2 \ln(2) \sqrt{P_{T_{2,2}}^{[k]} (\Psi_k)}} = 0 \quad (22a)$$

$$\delta_1 \left[2K\bar{q}_1 - \sum_{k=1}^K \log_2 (\Psi_k) \right] = 0 \quad (22b)$$

$$\delta_1 \geq 0 \quad (22c)$$

$$P_{T_{2,2}}^{[k]} \geq 0 \quad (22d)$$

Proposition 4: The problem (21a)–(21c) becomes convex with the condition of $\{P_{T_{2,2}}^{[k]} | P_{T_{2,2}}^{[k]} \geq 0\}$. When $\delta_1 > 0$, the LHS of (22a)–(22b) are monotone functions of $P_{T_{2,2}}^{[k]}$. Once again, a bi-section search algorithm may be used to solve (22a)–(22d), which is also the solution of the problem (21a)–(21c).

E. AO Algorithm

Based on the discussion in the Sections III-A to III-D, the proposed AO algorithm is summarized in Table I for solving the problem (14a)–(14d). Since the globally optimal solution is obtained for each subproblem, the proposed AO algorithm converges at least to a Nash point [24]. In our problem, although variables are coupled through the QoS constraints, according to [24] the AO algorithm still converges. The complexity of the AO algorithm is given by $O(cK(\kappa_1 + \kappa_2 + \kappa_3 + \kappa_4))$, where c is the number of iterations in the AO algorithm, $\kappa_1, \kappa_2, \kappa_3$, and κ_4 are the number of iterations in the bi-sections in each subproblem.

IV. NUMERICAL SIMULATIONS

A three-node two-way relay-assisted PLC system is shown in Fig. 2, where each segment of the network uses the same cable type. The cable parameters are shown in Table II [25]. Note that $R = R_0 \sqrt{f}$ and $G = 5G_0 \times 2\pi f$. The simulation parameters are set according to the physical layer specification of the HomePlug AV standard [26], [27].

TABLE I
AO ALGORITHM TO SOLVE THE OPTIMIZATION PROBLEM (22)–(25)

1) Initialize $P_{T_1}^{[1]}$, $P_{T_{2,1}}^{[1]}$ and $P_{T_{2,2}}^{[1]}$ as $p_{T_1,1}$, $p_{T_{2,1},1}$ and $p_{T_{2,2},1}$ with $P_{T_1}^{[k]} = 0$, $P_{T_{2,1}}^{[k]} = 0$ and $P_{T_{2,2}}^{[k]} = 0$, respectively for $k = 2, 3, \dots, K$.
2) Optimise $P_R^{[k]}$ with the previous $P_{T_1}^{[k]}$, $P_{T_{2,1}}^{[k]}$ and $P_{T_{2,2}}^{[k]}$ by solving (38)–(42).
3) Optimise $P_{T_1}^{[k]}$ with the newly optimized $P_R^{[k]}$ and the previous $P_{T_{2,1}}^{[k]}$ and $P_{T_{2,2}}^{[k]}$ by solving (57)–(61).
4) Optimise $P_{T_{2,1}}^{[k]}$ with the newly optimized $P_R^{[k]}$ and $P_{T_1}^{[k]}$ and the previous $P_{T_{2,2}}^{[k]}$ by solving (75)–(79).
5) Optimise $P_{T_{2,2}}^{[k]}$ with the newly optimized $P_R^{[k]}$, $P_{T_1}^{[k]}$ and $P_{T_{2,1}}^{[k]}$ by solving (86)–(89).
6) Calculate the total power (2) using with the obtained power allocation values.
7) Repeat Step 2 to Step 5 until convergence, i.e., the difference between the total power obtained in two successive iterations is less than a present threshold.

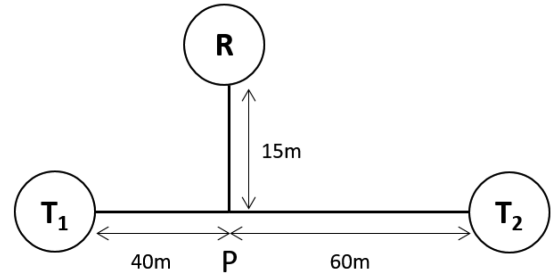


Fig. 2. Topology of a three-node two-way channel.

TABLE II
CHARACTERISTICS OF INDOOR POWER NETWORK CABLE

Parameter	Description	Value
R_0	resistance constant	9.34×10^{-5}
L	inductance per-unit-length	0.96×10^{-6}
C	capacitance per-unit-length	17.5×10^{-12}
G_0	conductance constant	34.7×10^{-14}

The noise of the PLC system is modelled as filtered white Gaussian noise (colored noise) as presented in [28], [29]. The noise at different nodes of the network is assumed to be independent and identically distributed (i.i.d.) and share the common PSD as shown in Fig. 3.

The source node has an inner impedance of $Z_S = 50\Omega$ in the transmit mode and load impedance $Z_l = 150\Omega$ in the receive mode. Meanwhile, the relay node has an inner impedance of $Z_{SR} = 50\Omega$ in the transmit mode and load impedance of $Z_{LR} = 150\Omega$ in the receive mode. The relay is attached to the branch where the preexisting load Z_b has the characteristics as shown in Fig. 4. The parameters for the preexisting load are shown in Table III [25].

The channel transfer functions of the relay-assisted PLC system in Fig. 2 are found by dividing it into several groups of the equivalent P2P PLC channel which adopt the Canate's channel model discussed in [25]. By configuring the parameters used for the P2P channel, a group of correlated path gains can be generated as depicted in Fig. 5. The normalized path gains

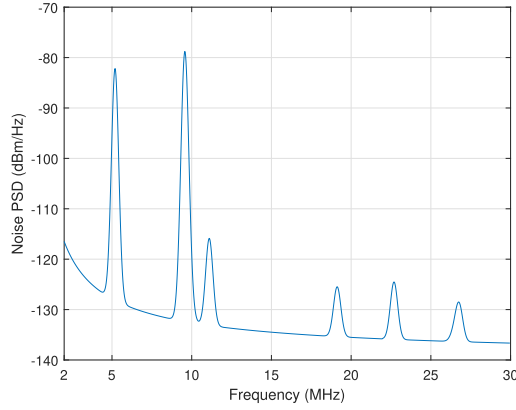
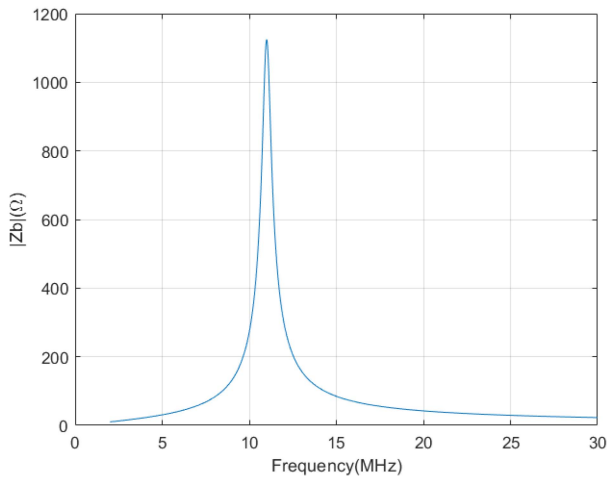


Fig. 3. PSD of the noise in a PLC system.

Fig. 4. Frequency response of preexisting load Z_b .TABLE III
PARAMETERS OF THE PREEXISTING LOAD, Z_b

Parameter	Description
Resistance	$R' \in \{200, 1800\}\Omega$ with a uniform distribution
Resonant frequency	$\omega_0/2\pi \in \{2, 28\}MHz$ with a uniform distribution
Q factor	$Q \in \{5, 25\}$ with a uniform distribution

on each sub-carrier are calculated and the results are shown in Fig. 6.

In this simulation, as shown in Table IV, we assume there are a total of $K = 1155$ OFDM subcarriers within the frequency band of 2 MHz to 30 MHz. The simulation results are generated by the proposed iterative algorithm where the convergence condition is specified as the difference between the total power obtained in two successive iterations being less than 10^{-5} .

We aim to obtain the minimal total power while satisfying the minimal ASC requirement. In the simulations, \bar{q}_2 is set to 2 bits/s/Hz and \bar{q}_1 is varied from 1.0 to 4.0 bits/s/Hz. Fig. 7 shows the total transmission power versus the number of iterations. It

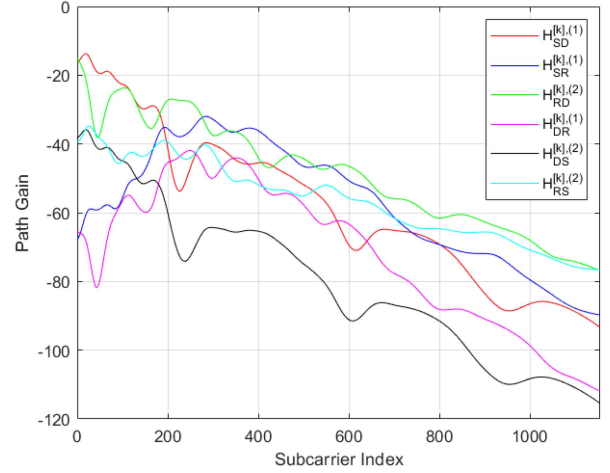


Fig. 5. Path gain of a three-node two-way relay system.

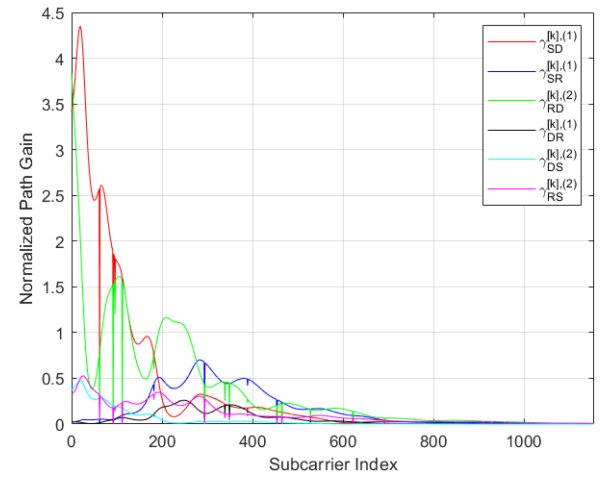


Fig. 6. Normalized path gain of a three-node two-way relay system.

TABLE IV
SYSTEM PARAMETERS USED FOR SIMULATION

Frequency band	2MHz - 30MHz
Total number of OFDM subcarriers	$K=1155$
Signalling path gain $\tilde{H}^{[k],(n)}$	Fig. 5
General background noise $N^{[k],(n)}$	Fig. 3
Normalised path gains $\gamma^{[k],(n)}$	Fig. 6

can be seen that the proposed AO algorithm converges within six iterations for $\bar{q}_1 = 1$. We note that for other values of \bar{q}_1 since the decrease of the total power is very small after six iterations, the good performance of the AO algorithm can be achieved with only a few iterations. This also shows that the AO algorithm has a short processing delay, which can fulfil the requirement of practical relay PLC systems. It is obvious that increasing the minimal ASC requirement needs more transmission power to meet the QoS constraint.

We also compare the AO algorithm with the well-known Expectation-Maximization (EM) algorithm [30], [31]. The details of the EM algorithm are given in Appendix D. It can be

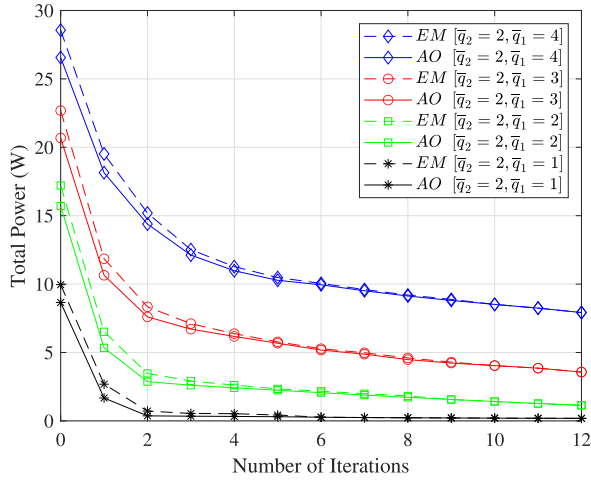


Fig. 7. Total power versus the number of iterations.

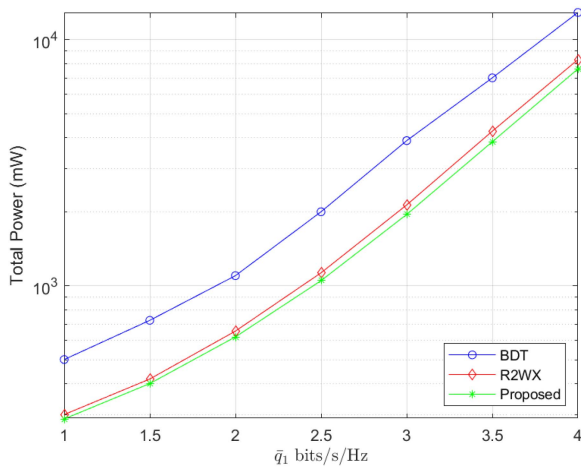


Fig. 8. Total power versus one directional ASC, \bar{q}_1 .

seen that both algorithms converge to the same point and the AO converges faster.

Further, the proposed scheme is compared with the conventional BDT system and relay-assisted two-way information exchange (R2WX) system under the same PLC configuration system. The conventional BDT system is configured such that in the first phase, the source node T_1 sends $X_1^{[k]}$ ($k = 1, 2, \dots, K$) signal with power $P_{T_1}^{[k]}$ to the destination node subjecting to the directional QoS constraints. In the second phase, the destination node T_2 replies $X_2^{[k]}$ ($k = 1, 2, \dots, K$) signal with power $P_{T_2}^{[k]}$ to the source node subjecting to the QoS requirement on the traffic direction. To meet the ASC constraint on the traffic direction, the power allocations at T_1 and T_2 use the water-filling algorithm [32]. Meanwhile, the R2WX system in [14] is configured such that in the first phase, the source node T_1 sends $X_1^{[k]}$ ($k = 1, 2, \dots, K$) signal with power $P_{T_1}^{[k]}$ to the relay node and at the same time, the destination node T_2 sends $X_2^{[k]}$ ($k = 1, 2, \dots, K$) signal with power $P_{T_2}^{[k]}$ to the relay node. In the second phase, the relay node amplifies the received signal

with amplitude gain and then broadcasts the amplified signal to the node T_1 and T_2 .

The total power versus the QoS constraints plots for the BDT system, the R2WX system and the proposed system are shown in Fig. 8. Furthermore, the simulation results show that the proposed system consumes about 40% less total power than the conventional BDT system to meet the same QoS requirements. Moreover, compared with the proposed system, the R2WX system needs more total power as the direct link between the source and destination nodes is not considered. In short, the proposed system consumes less power compared to the R2WX system proposed in [14].

V. CONCLUSION

We have derived the mathematical expressions of the three-node two-way PLC system to obtain the optimal power allocations. The AO algorithm has been employed to solve the optimization problem. The minimal channel capacity requirement has been applied to the PLC applications to examine the total transmission power minimization. The simulation results show that the AO algorithm converges in only a few iterations, which indicates that the AO algorithm has a short processing delay. The minimal transmission power increases with the ASC requirement as more transmission power is needed to meet the QoS constraint. Simulation results have shown that our method is able to make the system attain the same QoS requirements with less total power compared with the BDT system and the R2WX system.

APPENDIX

A Derivation of SNR_{T_1}

The received signal at T_1 in the second phase is given in (8). Since T_1 has full knowledge of $X_1^{[k]}$ and the channels, the first term of (8) can be eliminated. After elimination it becomes

$$\hat{Y}_{T_{1,2}}^{[k]} = (\xi + \varsigma)X_2^{[k]} + H_{RT_1}^{[k],(2)}g^{[k]}N_R^{[k]} + N_{T_1}^{[k]}, \quad (23)$$

where $\xi = H_{T_2R}^{[k],(1)}H_{RT_1}^{[k],(2)}g^{[k]}\sqrt{P_{T_{2,1}}^{[k]}}$, and $\varsigma = H_{T_2T_1}^{[k],(2)}\sqrt{P_{T_{2,2}}^{[k]}}$.

The power of signal at T_1 is given by

$$P_{T_1} = E \left\{ |(\xi + \varsigma)X_2^{[k]}|^2 \right\} = \left(|\xi|^2 + |\varsigma|^2 + 2\sqrt{|\xi|^2|\varsigma|^2} \right) E \left\{ |X_2^{[k]}|^2 \right\}, \quad (24)$$

where

$$|\xi|^2 = \frac{P_R^{[k]}P_{T_{2,1}}^{[k]}|H_{T_2R}^{[k],(1)}|^2|H_{RT_1}^{[k],(2)}|^2}{P_{T_1}^{[k]}|H_{T_1R}^{[k],(1)}|^2 + P_{T_{2,1}}^{[k]}|H_{T_2R}^{[k],(1)}|^2 + W^{[k]}},$$

$$|\varsigma|^2 = P_{T_{2,2}}^{[k]}|H_{T_2T_1}^{[k],(2)}|^2.$$

Note that $E\{|X_2^{[k]}|^2\} = 1$. For the sake of simplicity, we normalize the channel power to the noise power $W^{[k]}$. Therefore, we have the following:

$$\tilde{P}_{T_1} = |\xi|_N^2 + |s|_N^2 + 2\sqrt{|\xi|_N^2 |s|_N^2}, \quad (25)$$

where

$$|\xi|_N^2 = \frac{P_R^{[k]} P_{T_{2,1}}^{[k]} \lambda_{T_2 R}^{[k],(1)} \lambda_{RT_1}^{[k],(2)} W^{[k]}}{1 + P_{T_1}^{[k]} \lambda_{T_1 R}^{[k],(1)} + P_{T_{2,1}}^{[k]} \lambda_{T_2 R}^{[k],(1)}}, \quad (26)$$

$$|s|_N^2 = P_{T_{2,2}}^{[k]} \lambda_{T_2 T_1}^{[k],(2)} W^{[k]}, \quad (27)$$

and

$$\lambda_{L_1 L_2}^{[k],(n)} = \frac{|H_{L_1 L_2}^{[k],(n)}|^2}{W^{[k]}} \quad (28)$$

is the normalized path gain from node L_1 to L_2 in the n -th ($n = 1, 2$) phase. The power of noise at T_1 is given by

$$\begin{aligned} P_{N_{T_1}} &= E\left\{|H_{RT_1}^{[k],(2)} g^{[k]} N_R^{[k]}|^2\right\} + E\left\{|N_{T_1}^{[k]}|^2\right\} \\ &= |H_{RT_1}^{[k],(2)}|^2 |g^{[k]}|^2 E\left\{|N_R^{[k]}|^2\right\} + E\left\{|N_{T_1}^{[k]}|^2\right\}. \end{aligned}$$

Keep in mind that we assume that the power of noise is the same at each node for two successive phases. Thus, $E\{|N_R^{[k]}|^2\} = E\{|N_{T_1}^{[k]}|^2\} = W^{[k]}$. Similar to the signal power, after using (7) and normalizing the channel power, it becomes

$$\tilde{P}_{N_{T_1}} = \frac{P_R^{[k]} \lambda_{RT_1}^{[k],(2)} W^{[k]}}{1 + P_{T_1}^{[k]} \lambda_{T_1 R}^{[k],(1)} + P_{T_{2,1}}^{[k]} \lambda_{T_2 R}^{[k],(1)}} + W^{[k]}. \quad (29)$$

Finally, the SNR at node T_1 can be calculated as given in (30), shown as the bottom of this page.

B. Derivation of $SNR_{T_{2,1}}$

Similarly to the approach in Appendix A, the received signal at T_2 in the first phase becomes

$$\hat{Y}_{T_{2,1}}^{[k]} = \psi X_1^{[k]} + N_{T_{2,1}}^{[k]}, \quad (31)$$

where

$$\psi = H_{T_1 T_2}^{[k],(1)} \sqrt{P_{T_1}^{[k]}}. \quad (32)$$

The power of signal is given by

$$\begin{aligned} P_{T_{2,1}} &= E\left\{|\psi X_1^{[k]}|^2\right\} \\ &= |\psi|^2 E\left\{|X_1^{[k]}|^2\right\}, \end{aligned} \quad (33)$$

where

$$|\psi|^2 = P_{T_1}^{[k]} |H_{T_1 T_2}^{[k],(1)}|^2. \quad (34)$$

After normalizing the signal power, we have the following:

$$\tilde{P}_{T_{2,1}} = P_{T_1}^{[k]} \lambda_{T_1 T_2}^{[k],(1)} W^{[k]}. \quad (35)$$

The power of noise at T_2 during the first phase is given by

$$P_{N_{T_{2,1}}} = E\left\{|N_{T_{2,1}}^{[k]}|^2\right\}. \quad (36)$$

With the same assumption in Appendix A, the normalized noise power at T_2 during the first phase is given by

$$\tilde{P}_{N_{T_{2,1}}} = W^{[k]}. \quad (37)$$

The SNR at T_2 in the first phase can be calculated as

$$\begin{aligned} SNR_{T_{2,1}} &= \frac{\tilde{P}_{T_{2,1}}}{\tilde{P}_{N_{T_{2,1}}}} \\ &= P_{T_1}^{[k]} \lambda_{T_1 T_2}^{[k],(1)}. \end{aligned} \quad (38)$$

C. Derivation of $SNR_{T_{2,2}}$

The received signal at T_2 in the second phase becomes

$$\hat{Y}_{T_{2,2}}^{[k]} = \iota X_1^{[k]} + H_{RT_2}^{[k],(2)} g^{[k]} N_R^{[k]} + N_{T_2}^{[k]}, \quad (39)$$

where

$$\iota = H_{T_1 R}^{[k],(1)} H_{RT_2}^{[k],(2)} g^{[k]} \sqrt{P_{T_1}^{[k]}}, \quad (40)$$

and $g^{[k]}$ is given in (7). The power of signal is given by

$$\begin{aligned} P_{T_{2,2}} &= E\left\{|\iota X_1^{[k]}|^2\right\} \\ &= |\iota|^2 E\left\{|X_1^{[k]}|^2\right\}, \end{aligned} \quad (41)$$

where

$$|\iota|^2 = \frac{P_R^{[k]} P_{T_1}^{[k]} |H_{T_1 R}^{[k],(1)}|^2 |H_{RT_2}^{[k],(2)}|^2}{P_{T_1}^{[k]} |H_{T_1 R}^{[k],(1)}|^2 + P_{T_{2,1}}^{[k]} |H_{T_2 R}^{[k],(1)}|^2 + W^{[k]}}. \quad (42)$$

After normalizing the signal power, we have the following:

$$\tilde{P}_{T_{2,2}} = \frac{P_R^{[k]} P_{T_1}^{[k]} \lambda_{T_1 R}^{[k],(1)} \lambda_{RT_2}^{[k],(2)} W^{[k]}}{P_{T_1}^{[k]} \lambda_{T_1 R}^{[k],(1)} + P_{T_{2,1}}^{[k]} \lambda_{T_2 R}^{[k],(1)} + 1}. \quad (43)$$

The power of noise at T_2 during the second phase is given by

$$\begin{aligned} P_{N_{T_{2,2}}} &= E\left\{|H_{RT_2}^{[k],(2)} g^{[k]} N_R^{[k]}|^2\right\} + E\left\{|N_{T_2}^{[k]}|^2\right\} \\ &= |H_{RT_2}^{[k],(2)}|^2 |g^{[k]}|^2 E\left\{|N_R^{[k]}|^2\right\} + E\left\{|N_{T_2}^{[k]}|^2\right\} \end{aligned}$$

With the same assumption in Appendix A, the normalized noise power at T_2 during the second phase is given by

$$\tilde{P}_{N_{T_{2,2}}} = \frac{P_R^{[k]} \lambda_{RT_2}^{[k],(2)} W^{[k]}}{P_{T_1}^{[k]} \lambda_{T_1 R}^{[k],(1)} + P_{T_{2,1}}^{[k]} \lambda_{T_2 R}^{[k],(1)} + 1} + W^{[k]} \quad (44)$$

$$\begin{aligned} SNR_{T_1} &= \frac{\tilde{P}_{T_1}}{\tilde{P}_{N_{T_1}}} \\ &= \frac{\left(\sqrt{P_R^{[k]} \lambda_{RT_1}^{[k],(2)} P_{T_{2,1}}^{[k]} \lambda_{T_2 R}^{[k],(1)}} + \sqrt{P_{T_{2,2}}^{[k]} \lambda_{T_2 T_1}^{[k],(2)} \left(1 + P_{T_1}^{[k]} \lambda_{T_1 R}^{[k],(1)} + P_{T_{2,1}}^{[k]} \lambda_{T_2 R}^{[k],(1)}\right)}\right)^2}{1 + P_{T_1}^{[k]} \lambda_{T_1 R}^{[k],(1)} + P_{T_{2,1}}^{[k]} \lambda_{T_2 R}^{[k],(1)} + P_R^{[k]} \lambda_{RT_1}^{[k],(2)}} \end{aligned} \quad (30)$$

TABLE V
EM ALGORITHM TO SOLVE THE OPTIMIZATION PROBLEM

1) Set $t = 0$ and a feasible power for $P_R^{[k],(t)}$, $P_{T_1}^{[k],(t)}$, $P_{T_2}^{[k],(t)}$.
2) Set $t = t + 1$, using $P_{T_1}^{[k],(t)}$, $P_{T_2}^{[k],(t)}$ to obtain $P_R^{[k],(t+1)}$.
3) Using $P_{T_2}^{[k],(t)}$, $P_R^{[k],(t+1)}$ from step 2 to obtain $P_{T_1}^{[k],(t+1)}$.
4) Using $P_R^{[k],(t+1)}$, $P_{T_1}^{[k],(t+1)}$ from step 2 and step 3 to obtain $P_{T_2}^{[k],(t+1)}$.
5) If $\ P_R^{[k],(t+1)} - P_R^{[k],(t)}\ \leq \varepsilon$, $\ P_{T_1}^{[k],(t+1)} - P_{T_1}^{[k],(t)}\ \leq \varepsilon$, and $\ P_{T_2}^{[k],(t+1)} - P_{T_2}^{[k],(t)}\ \leq \varepsilon$ are satisfied, go to step 6. Otherwise, go to step 2.
6) Calculate the total power (2) using the obtained power allocation values.

The SNR at the destination node during the second phase can be calculated as given in (45).

$$\begin{aligned} SNR_{T_2,2} &= \frac{\tilde{P}_{T_2,2}}{\tilde{P}_{N_{T_2,2}}} \\ &= \frac{P_R^{[k]} \lambda_{RT_2}^{[k],(2)} P_{T_1}^{[k]} \lambda_{T_1R}^{[k],(1)}}{1 + \xi_k}, \end{aligned} \quad (45)$$

where

$$\xi_k = P_{T_1}^{[k]} \lambda_{T_1R}^{[k],(1)} + P_{T_2,1}^{[k]} \lambda_{T_2R}^{[k],(1)} + P_R^{[k]} \lambda_{RT_2}^{[k],(2)}.$$

D. EM Algorithm

In the presence of missing or hidden data, the EM algorithm can be used to iteratively compute the maximum likelihood (ML) estimate. In the EM algorithm, there are two steps involved: the E-step and the M-step. The power allocation optimization problems (14a)–(14d) can be formulated as

$$J(P_{T_1}^{[k]}, P_{T_2}^{[k]}, P_R^{[k]}) = \min_{P_{T_1}^{[k]}, P_{T_2}^{[k]}, P_R^{[k]}} P_\Sigma \quad (46)$$

subject to

$$\begin{aligned} \bar{C}_1 &\geq \bar{q}_1, \\ \bar{C}_2 &\geq \bar{q}_2, \\ P_{T_1}^{[k]}, P_{T_2}^{[k]}, P_R^{[k]} &\geq 0, \quad \forall k. \end{aligned}$$

For the objective function (46), using the EM algorithm, the power allocation problem can be formulated as

E-Step:

$$P_R^{[k],(t+1)} = \arg \min_{P_R^{[k]}} J(P_{T_1}^{[k],(t)}, P_{T_2}^{[k],(t)}, P_R^{[k]}) \quad (47)$$

M-Step:

$$P_{T_1}^{[k],(t+1)} = \arg \min_{P_{T_1}^{[k]}} J(P_{T_1}^{[k]}, P_{T_2}^{[k],(t)}, P_R^{[k],(t+1)}) \quad (48)$$

$$P_{T_2}^{[k],(t+1)} = \arg \min_{P_{T_2}^{[k]}} J(P_{T_1}^{[k],(t+1)}, P_{T_2}^{[k]}, P_R^{[k],(t+1)}) \quad (49)$$

By using the E-step and M-step above iteratively, we can obtain the solution for the objective function $J(P_{T_1}^{[k]}, P_{T_2}^{[k]}, P_R^{[k]})$. In Table V, the EM algorithm is summarized.

REFERENCES

- [1] T. A. Papadopoulos, C. G. Kaloudas, A. I. Chrysochos, and G. K. Papagiannis, "Application of narrowband power-line communication in medium-voltage smart distribution grids," *IEEE Trans. Power Del.*, vol. 28, no. 2, pp. 981–988, Apr. 2013.
- [2] G. Artale *et al.*, "A new low cost coupling system for power line communication on medium voltage smart grids," *IEEE Trans. Smart Grid*, vol. 9, no. 4, pp. 3321–3329, Jul. 2018.
- [3] Z. Fan *et al.*, "Smart grid communications: Overview of research challenges, solutions, and standardization activities," *IEEE Commun. Surv. Tut.*, vol. 15, no. 1, pp. 21–38, Jan.–Mar. 2013.
- [4] L. de M. B. A. Dib, V. Fernandes, M. de L. Filomeno, and M. V. Ribeiro, "Hybrid PLC/wireless communication for smart grids and Internet of Things applications," *IEEE Internet Things J.*, vol. 5, no. 2, pp. 655–667, Apr. 2018.
- [5] F. H. Juwono, Q. Guo, D. D. Huang, Y. Chen, L. Xu, and K. P. Wong, "On the performance of blanking nonlinearity in real-valued OFDM-based PLC," *IEEE Trans. Smart Grid*, vol. 9, no. 1, pp. 449–457, Jan. 2018.
- [6] A. Dubey and R. K. Mallik, "PLC system performance with AF relaying," *IEEE Trans. Commun.*, vol. 63, no. 6, pp. 2337–2345, Jun. 2015.
- [7] Y. Cao *et al.*, "Secrecy analysis for cooperative NOMA networks with multi-antenna full-duplex relay," *IEEE Trans. Commun.*, vol. 67, no. 8, pp. 5574–5587, Aug. 2019.
- [8] F. Cheng, G. Gui, N. Zhao, Y. Chen, J. Tang, and H. Sari, "UAV-relaying-assisted secure transmission with caching," *IEEE Trans. Commun.*, vol. 67, no. 5, pp. 3140–3153, May. 2019.
- [9] A. A. G. Liang, L. Gopal, F. H. Juwono, C. W. R. Chiong, and Y. Rong, "A channel model for three-node two-way relay-aided PLC systems," in *Proc. IEEE Int. Conf. Signal Image Process. Appl.*, 2019, pp. 52–57.
- [10] R. K. Ahiadormey, P. Anokye, H.-S. Jo, and K.-J. Lee, "Performance analysis of two-way relaying in cooperative power line communications," *IEEE Access*, vol. 7, pp. 97264–97280, 2019.
- [11] M. de Lima Filomeno, G. R. Colen, L. G. de Oliveira, and M. V. Ribeiro, "Two-stage single-relay channel model for in-home broadband PLC systems," *IEEE Syst. J.*, vol. 13, no. 1, pp. 204–214, Mar. 2019.
- [12] X. Wu and Y. Rong, "On the location of plug-in relay devices for indoor power line communication environment," in *Proc. 8th Int. Conf. Signal Process. Commun. Syst.*, 2014, pp. 1–6.
- [13] M. Noori and L. Lampe, "Improving data rate in relay-aided power line communications using network coding," in *Proc. IEEE Glob. Commun. Conf.*, 2013, pp. 2975–2980.
- [14] X. Wu and Y. Rong, "Joint terminals and relay optimization for two-way power line information exchange systems with QoS constraints," *EURASIP J. Adv. Signal Process.*, vol. 2015, no. 1, p. 84, Sep. 2015.
- [15] X. Wu and Y. Rong, "Optimal power allocation for non-regenerative multicarrier relay-assisted PLC systems with QoS constraints," in *Proc. IEEE Int. Symp. Power Line Commun. Appl.*, 2015, pp. 142–147.
- [16] X. Wu, B. Zhu, Y. Wang, and Y. Rong, "Optimization for relay-assisted broadband power line communication systems with QoS requirements under time-varying channel conditions," *KSII Trans. Internet Inf. Syst.*, vol. 11, pp. 4865–4886, 2017.
- [17] F. Jameel, Z. Hamid, F. Jabeen, S. Zeadally, and M. A. Javed, "A survey of device-to-device communications: Research issues and challenges," *IEEE Commun. Surv. Tut.*, vol. 20, no. 3, pp. 2133–2168, Jul.–Sep. 2018.
- [18] J. Joung and J. Choi, "Space-time line codes with power allocation for regenerative two-way relay systems," *IEEE Trans. Veh. Technol.*, vol. 68, no. 5, pp. 4884–4893, May 2019.
- [19] K. X. Nguyen, Y. Rong, and S. Nordholm, "MMSE-based joint source and relay optimization for interference MIMO relay systems," *EURASIP J. Wireless Commun. Netw.*, vol. 73, pp. 1–9, 2015.
- [20] G. Prasad and L. Lampe, "Full-duplex power line communications: Design and applications from multimedia to smart grid," *IEEE Commun. Mag.*, vol. 58, no. 2, pp. 106–112, Feb. 2020.
- [21] F. J. Cañete, G. Prasad, and L. Lampe, "PLC networks with in-band full-duplex relays," in *Proc. IEEE Int. Symp. Power Line Commun. Appl.*, 2020, pp. 1–6.
- [22] G. Prasad, L. Lampe, and S. Shekhar, "In-band full duplex broadband power line communications," *IEEE Trans. Commun.*, vol. 64, no. 9, pp. 3915–3931, Sep. 2016.
- [23] F. Passerini and A. M. Tonello, "Full duplex power line communication modems for network sensing," in *Proc. IEEE Int. Conf. Smart Grid Commun.*, 2017, pp. 213–217.

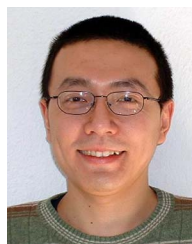
- [24] Y. Xu and W. Yin, "A block coordinate descent method for regularized multiconvex optimization with applications to nonnegative tensor factorization and completion," *SIAM J. Imag. Sci.*, vol. 6, no. 3, pp. 1758–1789, Sep. 2013.
- [25] F. J. Canete, J. A. Cortes, L. Diez, and J. T. Entrambasaguas, "A channel model proposal for indoor power line communications," *IEEE Commun. Mag.*, vol. 49, no. 12, pp. 166–174, Dec. 2011.
- [26] M. E. Hazen, "The technology behind homeplug AV powerline communications," *Computer*, vol. 41, no. 6, pp. 90–92, Jun. 2008.
- [27] L. Guerrieri, P. Bisaglia, G. Dell'Amico, and E. Guerrini, "Performance of the turbo coded HomePlug AV system over power-line channels," in *Proc. IEEE Int. Symp. Power Line Commun. Appl.*, 2007, pp. 138–143.
- [28] D. Benyoucef, "A new statistical model of the noise power density spectrum for powerline communication," in *Proc. IEEE Int. Symp. Power Line Commun. Appl.*, 2003, pp. 136–141.
- [29] T. Bai *et al.*, "Fifty years of noise modeling and mitigation in power-line communications," *IEEE Commun. Surv. Tut.*, vol. 23, no. 1, pp. 41–69, Oct.–Dec. 2021.
- [30] T. K. Moon, "The expectation-maximization algorithm," *IEEE Signal Process. Mag.*, vol. 13, no. 6, pp. 47–60, Nov. 1996.
- [31] F. Yuan, G.-P. Jin, L.-H. Zheng, and H. Ding, "Resource allocation for relay-assisted cognitive radio network with multiple channels," in *Proc. IEEE 11th Int. Conf. Signal Process.*, 2012, pp. 2217–2221.
- [32] N. Papandreou and T. Antonakopoulos, "Bit and power allocation in constrained multicarrier systems: The single-user case," *EURASIP J. Adv. Signal Process.*, vol. 6, pp. 1–14, 2008.



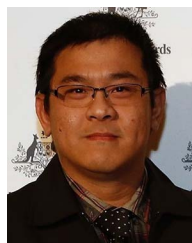
Angie A. G. Liong (Student Member, IEEE) received the bachelor's degree in electronic and communication engineering and the Ph.D. degree from Curtin University Malaysia, Miri, Malaysia, in 2014 and 2021, respectively. Her research interests include signal processing, power line communications, and channel modelling for PLC systems.



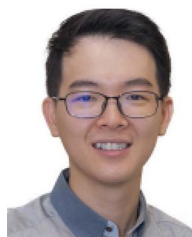
with the University of Southampton Malaysia, Iskandar Puteri, Malaysia. His research interests include signal processing for communications, power line communications, and the Internet of Things (IoT).



Yue Rong (Senior Member, IEEE) received the Ph.D. degree (*summa cum laude*) in electrical engineering from the Darmstadt University of Technology, Darmstadt, Germany, in 2005. He was a Postdoctoral Researcher with the Department of Electrical Engineering, University of California, Riverside, Riverside, CA, USA, from February 2006 to November 2007. Since December 2007, he has been with Curtin University, Bentley, WA, Australia, where he is currently a Professor. He has authored or coauthored more than 190 journal and conference papers in these areas. His research interests include signal processing for communications, wireless communications, underwater acoustic communications, underwater optical wireless communications, applications of linear algebra and optimization methods, and statistical and array signal processing. Dr. Rong was the recipient of the Best Paper Award at the 2011 International Conference on Wireless Communications and Signal Processing, the Best Paper Award at the 2010 Asia-Pacific Conference on Communications, and the Young Researcher of the Year Award of the Faculty of Science and Engineering at Curtin University in 2010. He is a Senior Area Editor of the IEEE TRANSACTIONS ON SIGNAL PROCESSING, and was an Associate Editor for the IEEE TRANSACTIONS ON SIGNAL PROCESSING from 2014 to 2018, the Editor of the IEEE WIRELESS COMMUNICATIONS LETTERS from 2012 to 2014, and the Guest Editor of the IEEE JOURNAL ON SELECTED AREAS IN COMMUNICATIONS special issue on theories and methods for advanced wireless relays. He was also a TPC Member for the IEEE ICC, IEEE GlobalSIP, EUSIPCO, IEEE ICC, WCSP, IWCMC, and ChinaCom.



Filbert H. Juwono (Senior Member, IEEE) received the B.Eng. degree in electrical engineering and the M.Eng. degree in telecommunication engineering from the University of Indonesia, Depok, Indonesia, in 2007 and 2009, respectively, and the Ph.D. degree in electrical and electronic engineering from The University of Western Australia, Perth, WA, Australia, in 2017. He is currently a Senior Lecturer with the Department of Electrical and Computer Engineering, Curtin University Malaysia, Miri, Malaysia. His research interests include signal processing for communications, wireless communications, power-line communications, machine learning applications, and biomedical engineering. He was the recipient of the prestigious Australian Awards Scholarship, in 2012. He is an Associate Editor for IEEE ACCESS, a Review Editor for *Frontiers in Signal Processing*, and the Editor-in-Chief for a newly established journal *Green Intelligent Systems and Applications*.



Choo W. R. Chiong (Member, IEEE) received the B.E. (Hons.) and Ph.D. degrees in electrical engineering from Curtin University, Bentley, WA, Australia, in 2010 and 2015, respectively. He is currently a Senior Lecturer with the Department of Electrical and Computer Engineering, Curtin University Malaysia, Miri, Malaysia. His research interests include signal processing for communications and power system optimization.